Simultaneous monitoring of the destruction of stearic acid and generation of carbon dioxide by self-cleaning semiconductor photocatalytic films

Andrew Mills *, Jishun Wang

Department of Pure and Applied Chemistry, University of Strathclyde, Glasgow G1 1XL, UK

Abstract

The destruction of stearic acid (SA), the SA test, is a popular approach used to evaluate the activities of photocatalytic films. The destruction of SA via semiconductor photocatalysis is monitored simultaneously, using FT-IR spectroscopy, via the disappearance of SA and the appearance of CO_2. Sol–gel and P25 films of titania are used as the semiconductor photocatalytic self-cleaning films. A conversion factor is used of 9.7×10^{15} molecules of SA $cm^{-2} \equiv 1\,cm^{-1}$ integrated areas of the peaks in the FT-IR of SA over the range 2700–3000 cm^{-1}, which is three times that reported previously by others. As the SA disappeared the concomitant amount of CO_2 generated was >90% that expected throughout the photomineralisation process for the sol–gel titania film. In contrast, the slightly more active, and scattering, P25 titania films generated CO_2 levels that dipped as low as 69% during the course of the photoreaction, but eventually recovered to $\cong$100% that expected based on the amount of SA present. The importance of these results with respect to SA test and the evaluation of new and existing self-cleaning films are discussed briefly.
© 2006 Elsevier B.V. All rights reserved.

Keywords: Stearic acid; Semiconductor photocatalysis; FT-IR; Carbon dioxide

1. Introduction

Much of the early work on semiconductor photocatalysis focused on the destruction of myriad different organic pollutants by oxygen, sensitized by particles of titania, dispersed in aqueous solution [1–3], i.e.:

$$\text{organic} + O_2 \xrightarrow[h\upsilon \ge E_{bg}]{TiO_2} CO_2 + H_2O + \text{mineral acids} \qquad (1)$$
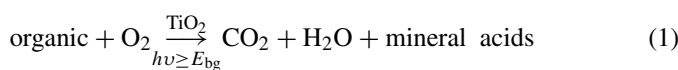
where E_{bg} is the bandgap of the semiconductor; $E_{bg} \cong$ 3.0–3.2 eV for TiO_2.

This work was partially spurred on by the possibility that semiconductor photocatalysis could be used as a method of purifying water. However, the scaling up of reaction (1) for such purposes has not proved simple, involving as it does the often use of artificial UV light sources and photocatalyst particle filtration and subsequent recovery steps [4,5]. As a consequence, the use of semiconductor photocatalysis in water purification has met with only limited commercial success to date [4,5].

In contrast, the use of reaction (1) as a way to create self-cleaning surfaces, such as glass, tiles, and tent fabric, has led to the creation of many large and successful commercial products [4,6–8]. The biggest of these is self-cleaning glass, which is produced by many of the major glass manufacturers, such as Pilkington Glass (Activ™) [6], St-Gobain (Bioclean™) [7] and PPG (SunClean™) [8]. With these and most other self-cleaning photocatalytic surfaces the active component is a surface layer of titania.

The generally preferred method for assessing the activity of a self-cleaning titania photocatalyst film is the stearic acid (SA) test, in which a thin layer of SA is deposited onto the film and its photocatalytic destruction monitored as a function of time [9–22]. This reaction has gained preference over the years for a number of reasons, including (a) SA provides a reasonable model compound for the solid films that deposit on exterior and interior surfaces, (b) SA is very stable under UV illumination in the absence of a photocatalyst film, (c) SA films, typically > monolayer i.e. >2.5 nm thick, are very easily laid down from a methanol or chloroform solution, (d) the kinetics of removal of SA are usually simple and zero-order, and so SA film thickness is not usually a critical factor when assessing photocatalytic activity, making the test much easier and (e) there

are many possible ways in which the mineralisation process can be monitored (vide infra).

The overall reaction can be summarized as follows:

$$CH_3(CH_2)_{16}CO_2H + 26O_2 \xrightarrow[h\upsilon \geq E_{bg}]{TiO_2} 18CO_2 + 18H_2O \qquad (2)$$
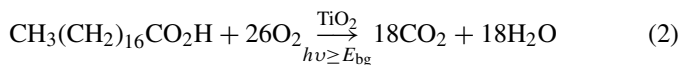
Following on from point (e) above, it is no surprise that this process has been studied a number of different ways including by monitoring: (i) the amount of CO_2 generated, using gas chromatography [13] and (ii) the change in thickness of the stearic acid film, using ellipsometry [18]. However, the most commonly employed method of studying reaction (2) is via the disappearance of the SA film using infrared absorption spectroscopy, since SA absorbs strongly in the region 2700–3000 cm^{-1}, with peaks at 2958 cm^{-1}, 2923 cm^{-1}, and 2853 cm^{-1}, due to asymmetric in-plane C–H stretching in the CH_3 group and asymmetric and symmetric C–H stretching in the CH_2 groups, respectively [9,12,20–22].

A brief inspection of reaction (2) reveals that the overall mineralization process involves the transfer of 104 electrons and this raises the question as to how the disappearance of SA and the generation of carbon dioxide are related? For example, Minabe et al. [13] have reported that the photocatalytic decomposition of SA sensitized by TiO_2 sol–gel, i.e. reaction (2), does not go to completion, but instead halts after ca. 69% of the compound has been decomposed. The implication of this work is that long-lived, recalcitrant oxidation intermediate products are formed that prevent reaction (2) going to completion and stop the SA:CO_2 stoichiometric ratio ultimately achieving the value of 1:18 indicated by reaction (2). If the findings of Minabe et al. [13] are correct, such a situation has serious implications with respect to self-cleaning glass products, and raises a number of important questions including, ultimately: is the SA test suitable for use as one of the methods, if not the method, of assessing the photocatalytic activity of self-cleaning films, commercial or otherwise?

Reassuringly, and in contrast to the work of Minabe et al. [13], others, including this group, have reported that sol–gel and CVD produced, titania films are able to completely remove SA via semiconductor photocatalysis [9,12,20–22]. However, none of these studies established that the simple reaction stoichiometry between SA and CO_2 is as indicated in reaction (2); a situation which most likely will only hold if any intermediates that are generated are non-volatile and more easily destroyed by semiconductor photocatalysis than the original SA.

The relationship between the level of SA removed and CO_2 generated via semiconductor photocatalysis could be most usefully studied if it were possible to monitor simultaneously the variations in both the levels of SA and CO_2 as a function of irradiation time. One way this could be achieved is by FT-IR spectroscopy using an IR gas cell with, as one of the two end-optical faces, a quartz disc, coated with a TiO_2 photocatalytic film with a top layer of SA, that faces into the sealed atmosphere of the gas cell. With such a system, irradiation of the SA/TiO_2 film optical face from the outside, with UV light capable of driving reaction (2), accompanied by the periodic measurement of the FT-IR absorption spectrum of the gas cell, would allow the disappearance of the SA film and the generation of any CO_2,

and any other IR-absorbing products, to be monitored simultaneously as a function of irradiation time using IR spectroscopy. In this paper the results of a study of reaction (2) based on such as system are described and the relationship between the level of SA removed and CO_2 generated assessed for two very different titania-based, photocatalytic films.

2. Experimental

Unless stated otherwise all chemicals were purchased from Aldrich Chemicals and were used as received. The 25 mm diameter (1 mm thick) quartz discs, used to support the SA/TiO_2 films and used as one of the end optical faces of a 10 cm IR gas cell (Lidam Scientific), were purchased from Newcastle Optics. The other end of the IR gas cell was a 25 mm diameter (2 mm thick) CaF_2 disc (Aldrich).

A typical Degussa P25 TiO_2 coated quartz disc was prepared by dipping the disc in a 5 wt.% P25 TiO_2 aqueous slurry then drying in an oven at 70 °C for 30 min. Loose material was then washed away using distilled water, the film blown dry using compressed air, and the process repeated three times until a titania film ca. 900 nm thick, as measured using a profilometer, was generated. Since the above procedure generates a titania film on both sides of the disc, and only one coated face was required, one of the disc faces (the outside face) was wiped clean of titania leaving a final film that was white and semi-transparent due to the P25 particles on the quartz disc.

A typical sol–gel film on a quartz disc was prepared using a TiO_2/carbowax paste, 14.5 wt.% TiO_2, the preparation details for which are given elsewhere [20]. 1 cm^3 of the paste was spread over the disc using a glass rod, allowed to dry in air and then annealed at 450 °C for 30 min. The final film was clear and colourless. BET analysis of the powder produced by scraping off the TiO_2 film, revealed a specific surface area of 80 $m^2 g^{-1}$. Porosity measurements indicated that the thick nanocrystalline films were largely mesopororous with an average porosity of 60%.

Stearic acid was deposited onto the two different titania films (i.e. P25 and sol–gel) by dropping 1 cm^3 of a 0.2 mol dm^{-3} SA in chloroform solution onto the disc and spinning at 2000 rpm for 1 min. The film was then further dried, and any loose material removed, by blowing compressed air over it for 1 min.

All UV/vis absorption spectra were recorded using a Perkin Elmer Lambda 20 spectrophotometer and all infrared absorption spectra were recorded using a Perkin Elmer Spectrum One FT-IR spectrometer.

All UV irradiations were carried out using six 8 W germicidal ($\lambda_{emission} = 254$ nm) fluorescent lamps set in a cylindrical hemisphere with an aluminium reflector. Typically the incident UV light intensity was 8.12 mW cm^{-2}, as measured using a calibrated UV meter (UVP model MS-100 with MS 125 UVC sensor).

3. Results and discussion

The UV/vis absorption spectra of the two titania films on quartz were recorded and the results are illustrated in Fig. 1. As
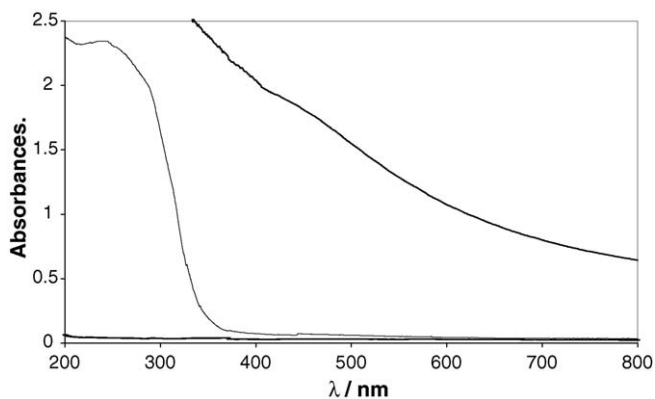
Fig. 1. UV/visible absorption spectra of P25 TiO$_2$ film (top bold line), sol–gel TiO$_2$ film (light line) and stearic acid film (bottom bold line) on quartz discs.

is typical of P25 titania, which is a 70:30 mixture of anatase and rutile, the spectrum is dominated by a strong background absorbance that increases with decreasing wavelength due to particle light scattering. Degussa P25 comprises ca. 32 nm particles that give it a specific surface area of ca. 55 m^2 g^{-1}, but most of these particles are fused together to form up to micron-sized aggregates and it is the latter that are responsible for the extensive light scattering exhibited by P25 aqueous dispersions and films [23]. In contrast, the sol–gel titania films comprise particles of ca. 10–15 nm diameter that do not form large aggregates and thus do not scatter visible light to any appreciable extent [20,21]. From its absorbance, at 254 nm (ca. 2.3) and the relationship, Abs$_\lambda$ = 0.434 $\alpha_\lambda d$ [22], where Abs$_\lambda$ is the absorbance of the film at wavelength λ and α_λ is the absorption coefficient of titania ($\alpha_{254} = 5.1 \times 10^5$ cm^{-1}), it is possible to estimate the thickness (d) of the sol–gel titania film to be ca. 104 nm, which compares well with the value of 110 nm measured using profilometry.

As noted earlier, the FT-IR spectrum of stearic acid exhibits a series of characteristic absorption peaks over the range 2700–3000 cm^{-1} and Paz et al. [9] were one of the first research groups to study reaction (2) using titania films, the SA test, and the FT-IR spectrum of SA to estimate the level of SA remaining on their films in units of molecules of SA cm^{-2}. In this work they *estimated* an integrated area under the FT-IR spectrum of SA of 0.6 cm^{-1} was due to ca. 1.9×10^{15} molecules of SA acid cm^{-2}, i.e. 3.2×10^{15} molecules of SA cm^{-2} is equivalent to an integrated FT-IR spectrum area value of 1 cm^{-1} [9]; throughout the rest of this paper we shall refer to this conversion factor as δ. In order to confirm the above value of δ in the current work, the integrated areas of a series of different levels/thicknesses of SA on titania and plain quartz were measured, along with the masses of each of the films, measured by weighing each film before and after the deposition of the SA. The plot of the results of this work in the form of the mass of stearic acid versus integrated area gave an excellent straight line ($r^2 = 0.9999$) with a gradient of 2.25×10^{-5} g/cm^{-1}; given that the area of the quartz discs used was 4.9 cm^2, and the molecular mass of SA = 284, it follows that the value of δ appears to be 9.7×10^{15} molecules of SA cm^{-2}. This measured value of δ is ca. three times larger than that estimated by Paz et al.

[9] and suggests that all future work on this system, in which FT-IR is used to assess the level of SA present, should use the much higher, measured, conversion value reported here, namely: 9.7×10^{15} molecules SA cm$^{-2} \equiv 1$ cm^{-1}, over the integration range 2700 (and 2800)–3000 cm^{-1}, rather then the previously estimated value [9].

The FT-IR spectrum of CO$_2$ in the gas cell was also recorded and found not to interfere with that of SA, spanning as it does the range 2250–2400 cm^{-1}, with peaks at 2357 and 2341 cm^{-1}, due to the asymmetric and symmetric stretching modes of CO$_2$. Calibration injections of different known volumes of CO$_2$ into the gas cell, accompanied by the measurement of the associated integrated peak areas in the FT-IR spectrum over the range 2250–2400 cm^{-1}, established the expected simple linear relationship between these two parameters. The proportionality constant derived from this work was then used in all subsequent work to calculate the number of moles of CO$_2$ present in the gas cell at any time during the course of an irradiation, based on the measured integrated area in the FT-IR spectrum over the wavenumber range 2250–2400 cm^{-1}.

In a typical experiment a SA–coated titania–quartz disc (either P25 titania or sol–gel titania film) was used as one of the windows of a 10 cm cylindrical FT-IR gas cell, with the SA/titania film facing inwards. The cell was flushed with air, sealed and the SA/titania film end irradiated with UVC light. The FT-IR absorption spectrum of the cell and its contents was measured periodically as the irradiation proceeded; a typical set spectra that resulted using a P25 titania film are illustrated in Fig. 2. From the data in Fig. 2 it is clear that as the SA film disappears, with peaks in the range 2700–3000 cm^{-1}, noticeable amounts of CO$_2$ are generated, with peaks in the range 2250–2400 cm^{-1} For each spectrum the integrated area under the SA absorption peaks was measured and a resulting plot of the number of molecules of SA versus irradiation time was generated. Similarly, for each spectrum in Fig. 2, the integrated area under the CO$_2$ absorption peaks was determined and a
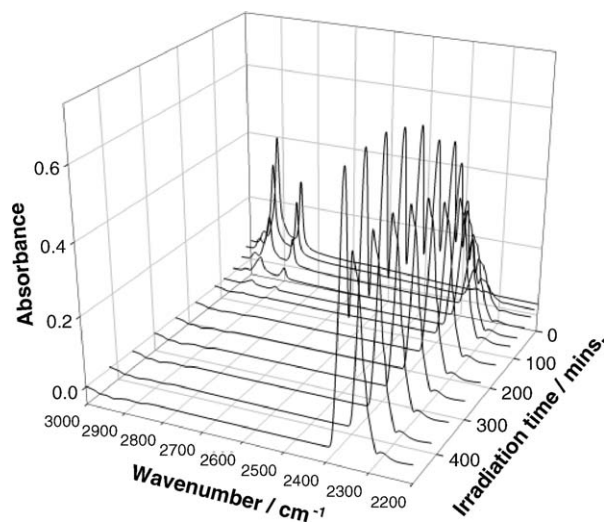

Fig. 2. FT-IR absorption spectra of the IR gas cell with a quartz window, coated with a P25 TiO$_2$ layer, which, in turn, was initially coated with a layer of stearic acid as a function of irradiation time.

plot of $(1/18) \times$ number of moles of CO_2 also generated. The multiplying factor of $(1/18)$ was used in order to allow the ready comparison of the number of moles of SA removed to the number of moles of CO_2 generated, see the stoichiometry in reaction (2). The results of this work for both the sol–gel and P25 titania films are illustrated in Fig. 3(a) and (b), respectively, and show that in both cases upon prolonged irradiation all the SA initially present is eventually converted to CO_2 and in a (1:18) reaction stoichiometry that supports that indicated in reaction (2).

In both Fig. 3(a) and (b) the sum of the measured numbers of moles of SA and CO_2 is represented by solid square data points and its variation as a function of irradiation time reveals that for the film with the slightly lower activity (sol–gel) the 1:18 relationship between SA and CO_2 is largely (>90%) preserved throughout the irradiation process, presumably because the many reaction intermediates associated with reaction (2) are more easily oxidized than SA itself. In contrast, from the results in Fig. 3(b) for the most active titania film (P25) the SA:CO_2 ratio appears to drop from an initial SA:CO_2 reaction stoichiometry value of 1:18 to a minimum of ca. 1:12, i.e. 69% of that expected, after ca. 50 min irradiation, before recovering to a ratio of 1:18 at the end of the process.

The likely cause for this loss of stoichiometry is the formation of intermediates that appear less easy to destroy. Similar negative deviations from the expected organic:CO_2 reaction stoichiometry ratio have been reported by others [1,2] in many semiconduc-

tor photomineralisation studies, including Romeas et al. [24] in their work on the photomineralisation of palmitic acid by TiO_2-coated self-cleaning glass. In the latter work [24], the major intermediates (ca. 22%) were found to be acetone, acetaldehyde and formaldehyde and these products may be the cause for the observed drop in the SA:CO_2 ratio from its expected value of 1:18 found here. However, careful examination of the FT-IR spectra revealed no evidence for these latter species, although this may have been due to adsorption and/or occlusion of these species on the very high surface area, porous aggregates of the P25 titania particles. It is also possible that the IR absorbance spectra of the intermediates are screened by the strong IR spectrum of the generated CO_2. However, the results of experiments carried out on the same system using an open cell revealed no evidence for any major adsorbed intermediates, implying that if such screening does occur, the intermediates must be volatile.

The SA decay data illustrated in Fig. 3 for SA can be used to calculate the initial formal quantum efficiency for the removal of SA, i.e. FQE(SA), by these two films where

$$FQE(SA) = \frac{\text{rate of removal of SA (molecules/s)}}{\text{rate of incident light (photons/s)}} \quad (3)$$

and the results of these calculations are given in Table 1. Upon initial inspection these calculated values appear significantly smaller than those reported previously for similar titania films. For example, after correcting for the low δ value used (vide supra), the work of Paz and co-workers reveals FQE(SA) values of 6.7×10^{-3} and 8.2×10^{-3} for sol–gel and P25 films that are 2.7 and 1.9 times bigger, respectively, than those reported here. However, in contrast to most other work on reaction (2), including that of Paz et al. [9], in this study irradiation of the TiO_2 film was through the back, rather than front, of the supporting glass substrate. Separate experiments carried out on the TiO_2/SA film system revealed that the rate of destruction was always lower if the back rather than the front face was irradi-
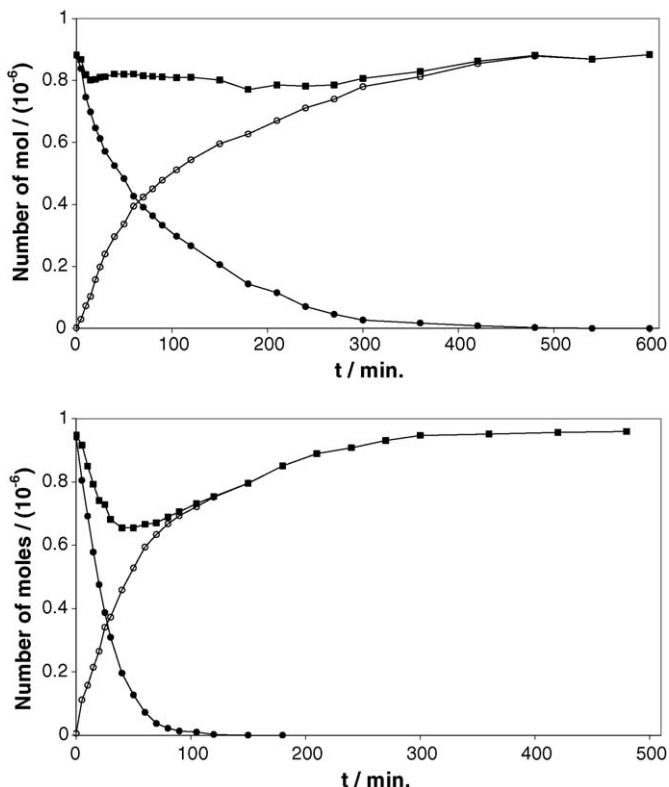

Fig. 3. Plots of the variations in: (i) the number of moles of stearic acid (●), (ii) $(1/18) \times$ the number of moles of CO_2 (○) and (iii) the sum of (i) and (ii) (■) as a function of irradiation time for (a) sol–gel TiO_2 film and (b) P25 TiO_2 film. The data for the plots was derived from the integrated areas under the IR peaks, such as shown in Fig. 2, and appropriate calibration plots.

Table 1
Calculated initial formal quantum efficiencies[a] for stearic acid removal (FQE(SA))

Key parameters	Sol–gel TiO_2 film[b]	P25 TiO_2 film
Initial SA disappearance rate (mol/min)	1.26×10^{-8}	2.41×10^{-8}
Incident light intensity (mW/cm^{-2})	8.12	8.12
Incident light intensity (No. of photons per second)	5.08×10^{16}	5.08×10^{16}
FQE(SA)/10^{-3}	2.5	4.8
Other FQE(SA) values		
Paz et al. [9]	6.7 (2.2)[c]	8.2 (2.7)[c]
Mills et al. [20–22]	4.5 (1.5)[c]	7.9 (2.6)[c]

[a] Formal quantum efficiency (FQE) = rate of photochemical process (mol/s)/intensity of incident light (photons/s).

[b] The FQE values reported for the sol–gel films are also *quantum yields*, since the films are non-scattering (i.e. clear) and have large (>2) absorbances at 254 nm so that the incident light intensity is also the absorbed incident light intensity.

[c] The FQE values in parentheses are those values reported by the authors using the *estimated* conversion factor of 1 cm$^{-1} \equiv 3.2 \times 10^{15}$ molecules of SA cm^{-2}. This work shows that the conversion factor should in fact be 9.7×10^{15} molecules of SA per cm^2. All FQEs *not* in parentheses therefore have been calculated using the latter *measured* value.

ated, presumably due to additional light reflection and scattering losses. Not surprisingly, given the absorption data illustrated in Fig. 1, the effect was most striking for the highly light-scattering P25 titania films. Thus, typically P25 films were found to exhibit initial SA photo-destruction rates that were 36% slower if irradiated from the back compared to the front. In contrast, the difference was only 13% for the less light-scattering paste titania films.

From the results in Table 1 it appears that P25 is initially able to remove SA and generate CO_2 via reaction (2) twice as fast as the sol–gel titania and although this may be due to differences in mechanism, the lack of measurable intermediates prevents any meaningful discussion in this regard. It is certainly not unusual for different samples of titania to exhibit different activities, and generate wildly different levels of intermediates, in the photocatalytic destruction of organics (e.g. [25,26]). An excellent example of this is provided by the work of Theurich et al. in their study of the photocatalytic destruction of 4-chlorophenol, 4-CP, by P25 and Hombikat UV 100 titania, which showed that a higher photonic efficiency is observed for P25, even though the latter generates higher levels of intermediates, in markedly different molar ratios [26]. Despite the fact that observed differences in photocatalytic rate for different samples of titania are not uncommon, and also depend upon the pollutant, the major cause for this remains unclear. Although it has been shown that such variations between titania samples are not simply related to bulk physical characteristics, such as degree of crystallinity, crystal phase or specific surface area [25], these parameters are obviously important in determining overall activity and should not be neglected. Thus, the difference in activity between P25 and sol–gel titania reported here may be simply related to differences in porosity and/or other, more complex, possibly mechanistic factors.

Although it was not possible to estimate the fraction of incident UVC light absorbed, by the P25 titania films, this was not the case for the sol–gel titania films (given, as noted earlier, Abs(254 nm) = 2.3 for this film). As a consequence, as indicated in Table 1, the FQE(SA) value reported for the sol–gel film is really a quantum yield and equal to 2.5×10^{-3} for back light irradiation. Given that the overall process involves 104 electrons, see reaction (2), and that for these films the typical reaction SA:CO_2 stoichiometry is >90% throughout the irradiation process, it would appear that the quantum yield for this process on an electron/photon basis is ca. >22% for back light irradiation. This value would be even higher (at least 36% higher; vide supra) if irradiated from the front and implies that the photocatalytic process reaction (2) on titania sol–gel films is actually quite efficient. For comparison, films of titania produced by CVD, including the commercial self-cleaning glass, Activ®, have been shown to exhibit quantum yields, and therefore electron/photon efficiencies, for reaction (2) that are 6–12 times less than that that of the titania sol–gel films used here [21]. Thus, the sol–gel films reported here are really very active and photon efficient with regard to semiconductor photocatalysis.

If SA is not a special case, and the above high efficiency of photomineralisation is also to be found using these films for the destruction of most other organic pollutants, then the photocatalytic mineralization of organics by titania films appears to represent a very attractive and efficient approach to providing clean surfaces. Assuming that irradiation of such films would utilise sunlight, rather than light from an artificial UV light source, then the only problem with such films appears to be the large value of the bandgap of titania (i.e. 3.0–3.2 eV) which means that little (<5%) of any incident sunlight would be absorbed by the films. The creation of a cheap, reproducible semiconductor material that has the photocatalytic properties of titania but can absorb a larger fraction of the solar spectrum is the current objective of many research groups and has met with very mixed success [27,28]. It appears likely that even if a reproducible, visible-light driven semiconductor photocatalyst can be created, its electron/photon efficiency for reaction (2) will be much less than it is for titania, due to its necessarily smaller bandgap and most likely less effective band positions. Whether this loss in efficiency is readily compensated by its greater overlap with the solar spectrum, leading to a greater efficacy, as a solar energy driven photocatalyst, remains to be seen. What is for certain is the accurate and reliable assessment of the activities of such films is essential if any real progress is to be made and the work reported here, on the photocatalytic destruction of SA, should help address this need.

References

[1] M.R. Hoffmann, S.T. Martin, W.Y. Choi, D.W. Bahnemann, Chem. Rev. 95 (1995) 69–96, and references therein.

[2] A.L. Linsebigler, G.Q. Lu, J.T. Yates, Chem. Rev. 95 (1995) 735–758, and references therein.

[3] A. Mills, S. LeHunte, J. Photochem. Photobiol. A: Chem. 108 (1997) 1–35.

[4] A. Mills, S.K. Lee, J. Photochem. Photobiol. A:Chem. 152 (2002) 233–247.

[5] S.K. Lee, A. Mills, J. Ind. Eng. Chem. 10 (2004) 173–187, and references therein.

[6] http://www.pilkington.com (accessed December 2005).

[7] http://www.saint-gobain-glass.com/fr/index.asp (accessed December 2005).

[8] http://www.ppg.com/gls_residential/gls_sunclean/ (accessed December 2005).

[9] Y. Paz, Z. Luo, L. Rabenberg, A. Heller, J. Mater. Res. 10 (1995) 2842–2848.

[10] R. Fretwell, P. Douglas, J. Photochem. Photobiol. A: Chem. 143 (2001) 229–240.

[11] Y. Paz, A. Heller, J. Mater. Res. 12 (1997) 2759–2766.

[12] T. Sawunyama, L. Jiang, A. Fujishima, K. Hashimoto, J. Phys. Chem. B. 101 (1997) 1100–11003.

[13] T. Minabe, D.A. Tryk, P. Sawunyama, Y. Kikuchi, K. Hashimoto, A. Fujishima, J. Photochem. Photobiol. A: Chem. 137 (2000) 53–62.

[14] T.D. Manning, I.P. Parkin, R.J.H. Clark, D. Sheel, M.E. Pemble, D. Vernadou, J. Mater. Chem. 12 (2002) 2936–2939.

[15] S. Lee, H.S. Jung, D.W. Kim, K.S. Hong, Mater. Sci. Forum 486/487 (2005) 65–68.

[16] M. Arbab, L.J. Shekstak, C.S. Harris, Am. Ceram. Bull. 84 (2005) 34–38.

[17] L. Frazer, Environ. Health Perspect. 109 (2001) 174–177.

[18] J.T. Remillard, J.R. McBride, K.E. Nietering, A.R. Drews, X. Zhang, J. Phys. Chem. B 104 (2000) 4440–4447.

[19] S. Sitkiewitz, A. Heller, New J. Chem. 20 (1996) 233–241.

[20] A. Mills, N. Elliott, G. Hill, D. Fallis, J.R. Durrant, R.L. Willis, Photochem. Photobiol. Sci. 2 (2003) 591–596.

[21] A. Mills, G. Hill, S. Bhopal, I.P. Parkin, S.A. O'Neill, J. Photochem. Photobiol. A: Chem. 160 (2003) 185–194.

[22] A. Mills, S.K. Lee, A. Lepre, I.P. Parkin, S.A. O'Neill, Photochem. Photobiol. Sci. 1 (2002) 865–868.

[23] M. Nargiello, T. Herz, in: D.F. Ollis, H. Al-Ekabi (Eds.), Photocatalytic Purification and Treatment of Water and Air, Elsevier, Amsterdam, 1993, pp. 801–807.

[24] V. Romeas, P. Pichat, C. Guillard, T. Chopin, C. Lehaut, New J. Chem. 23 (1999) 365–373.

[25] A. Mills, P. Sawunyama, J. Photochem. Photobiol. A: Chem. 84 (1994) 305–309.

[26] J. Theurich, M. Linder, D.W. Bahnemann, Langmuir 12 (1996) 6368–6376.

[27] R. Ashai, T. Morikawa, T. Ohwaki, K. Aoki, Y. Taga, Science 293 (2001) 269–271.

[28] M. Mrowetz, W. Balcerski, A.J. Colussi, M.R. Hoffmann, J. Phys. Chem. B 108 (2004) 17269–17273.